

ORIGINAL ARTICLE

Open Access



# Experimental study on the characteristic values of partial compression perpendicular to the grain of hardwood with edge distance parallel and perpendicular to the grain

Hiroto Suesada<sup>1\*</sup>  and Kohta Miyamoto<sup>2</sup>

## Abstract

Some hardwoods have a higher density and superior structural performance than softwoods, which are generally used as construction materials in buildings. Therefore, the characteristics of hardwoods are advantageous in their use for wooden joints. However, the effects of the dimensions of hardwood specimens and wood species on the partial compression performance perpendicular to the grain are unclear. In this study, we conducted partial compression tests perpendicular to the grain of hardwoods to clarify the effects of the edge distance and wood species on the characteristic values. The relationships between the partial compression performance perpendicular to the grain and the edge distance perpendicular to the grain of hardwoods were similar to those of softwoods. A significant correlation was observed between the density and the characteristic values of partial compression perpendicular to the grain. There were differences in the fracture morphologies and stress–strain curves between diffuse and ring-porous woods. However, factors other than density and whether the wood is diffuse- or ring-porous are responsible for the differences in the effect of the edge distance on the characteristic values between wood species.

**Keywords** Hardwood, Partial compression perpendicular to the grain, Edge distance parallel to the grain, Edge distance perpendicular to the grain, Fracture morphology

## Introduction

In Japan, most planted forests are in the mature and utilisation stages [2]. In addition, the environmental advantages of wooden buildings have increased in the number of mid-rise and large-scale nonresidential wooden buildings [1]. These buildings require higher structural performance than low-rise buildings [1].

One of the challenges in improving the structural performance of wooden buildings is controlling the compressive deformation of wood perpendicular to the grain at the joints. The compression performance of wood perpendicular to the grain was considerably lower than that of wood parallel to the grain [1]. In addition, partial compressive deformation of wood perpendicular to the grain occurs in nearly all joints in wooden buildings. Partial compressive deformation perpendicular to the grain is one of the primary causes of wooden joint deformation [1]. Therefore, to improve and control the structural performance of wooden joints, the use of wood with superior partial compression performance perpendicular to the grain is effective. Some hardwood species have a higher density and superior compression performance perpendicular to the grain compared to softwoods, which

\*Correspondence:

Hiroto Suesada  
suesada@shinshu-u.ac.jp

<sup>1</sup> Faculty of Agriculture, Shinshu University, Minamiminowa, Nagano 399-4598, Japan

<sup>2</sup> Forestry and Forest Products Research Institute, Matsunosato 1, Tsukuba, Ibaraki 305-8687, Japan



© The Author(s) 2024. **Open Access** This article is licensed under a Creative Commons Attribution 4.0 International License, which permits use, sharing, adaptation, distribution and reproduction in any medium or format, as long as you give appropriate credit to the original author(s) and the source, provide a link to the Creative Commons licence, and indicate if changes were made. The images or other third party material in this article are included in the article's Creative Commons licence, unless indicated otherwise in a credit line to the material. If material is not included in the article's Creative Commons licence and your intended use is not permitted by statutory regulation or exceeds the permitted use, you will need to obtain permission directly from the copyright holder. To view a copy of this licence, visit <http://creativecommons.org/licenses/by/4.0/>.

are generally used as construction materials in buildings [1]. Therefore, these hardwoods are advantageous for wooden joints. Estimating the performance of hardwoods is essential for their utilisation as structural materials but not for the partial compression performance of hardwoods perpendicular to the grain [1]. Furthermore, the effects of the dimensions of hardwood specimens and wood species on the partial compression performance perpendicular to the grain are unclear [1].

In Japan, the formula established by Inayama [e.g., 3–5] is commonly used to estimate partial compression performance perpendicular to grain [6]. However, whether this formula can be applied to hardwoods is unclear because these studies focused on softwood such as Japanese cedar and Douglas fir. Fujita [7] proposed a method for applying this formula to hardwoods. However, this method has only been validated for a limited variety of dimensions because it assumes hardwood is used for connectors.

The effects of hardwood dimensions, particularly the edge distance orthogonal to the longitudinal direction, on compression performance perpendicular to the grain have not been studied in detail. Therefore, in this study, partial compression tests perpendicular to the grain were conducted to clarify the effects of edge distances parallel and perpendicular to the grain and wood species on the characteristic values.

This paper reconstructs the previous study [1] with additional destruction forms and some data.

## Materials and methods

### Test specimens

Table 1 lists the specifications, densities and moisture contents of the test specimens. Eight Japanese hardwood species were used as the test specimens. Itayakaede (IT, *Acer mono* Maxim.), Udaikamba (UD, *Betula maximowicziana*), Buna (BN, *Fagus crenata*), and Shirakashi (SR, *Quercus myrsinifolia*) are diffuse-porous woods. Kuri (KR, *Castanea crenata*), Keyaki (KY, *Zelkova serrata*),

Yachidamo (YC, *Fraxinus mandshurica*), and Mizunara (MZ, *Quercus crispula* Blume) are ring-porous woods. Their fracture morphologies and stress–strain curve trends differed between the diffuse- and ring-porous wood. Buna clearly represented the typical characteristics in the diffuse-porous woods and Keyaki in the ring-porous woods. Therefore, in the Results and discussion section, Buna and Keyaki were selected as examples for the description of the diffuse- and ring-porous woods, respectively.

The height of each sample is fixed at 40 mm. Specimens with three different widths ( $w$ ) (40, 60, and 80 mm) and two different lengths ( $l$ ) (40 and 120 mm) were fabricated. Thus, each wood specimen had six-dimensional specifications indicated by a four-digit number. For example, 4040 represents a width of 40 mm and a length of 40 mm, whereas 6120 represents a width of 60 mm and a length of 120 mm. Three to six specimens are prepared for each specification. For each species, specimens of different widths and lengths were obtained from a single piece of wood in the continuous longitudinal direction to reduce the variation in materials and better clarify the effect of dimensions.

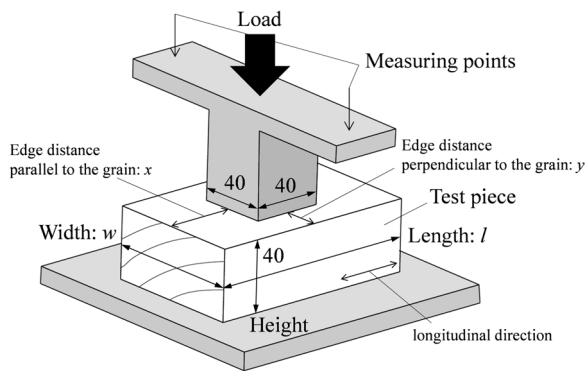
### Compression test perpendicular to the grain

Figure 1 shows a schematic of the partial compression test performed perpendicular to the grain. The tests were conducted in accordance with JIS Z 2101 [8]. Figure 1 shows the centre of the specimen loaded with a metal bearing plate with a length and width of 40 mm. Therefore, the edge distances parallel ( $x$ ) and perpendicular ( $y$ ) to the grain were represented by  $(l - 40)/2$  and  $(w - 40)/2$ , respectively. Accordingly,  $x$  is 0 mm (4040, 6040, 8040) and 40 mm (4120, 6120, 8120), and  $y$  is 0 mm (4040, 4120), 10 mm (6040, 6120) and 20 mm (8040, 8120). When both  $x$  and  $y$  were 0 mm (4040), full compression tests were performed perpendicular to the grain.

**Table 1** Specification of the test specimens [1]

Wood species	Length (mm)	Width (mm)	$n^a$	$\rho^{b,c}$ (kg/m <sup>3</sup> )	MC <sup>c,d</sup> (%)	AAR <sup>c,e</sup> (°)	ARW <sup>c,f</sup> (mm)
Itayakaede (IT, <i>Acer mono</i> Maxim.)	40/120	40/60/80	6	734 ± 32.8	10.9 ± 0.89	20.2 ± 11.3	3.06 ± 0.992
Shirakashi (SR, <i>Quercus myrsinifolia</i> )	40/120	40/60/80	3	890 ± 59.5	12.6 ± 0.20	43.6 ± 8.30	4.39 ± 0.535
Udaikamba (UD, <i>Betula maximowicziana</i> )	40/120	40/60/80	4	707 ± 71.9	12.1 ± 0.72	19.1 ± 8.93	1.61 ± 0.323
Kuri (KR, <i>Castanea crenata</i> )	40/120	40/60/80	6	575 ± 73.7	13.9 ± 0.88	35.0 ± 25.3	3.29 ± 1.34
Keyaki (KY, <i>Zelkova serrata</i> )	40/120	40/60/80	6	747 ± 67.7	12.2 ± 1.93	43.3 ± 24.8	4.21 ± 1.51
Yachidamo (YC, <i>Fraxinus mandshurica</i> )	40/120	40/60/80	6	571 ± 80.4	13.3 ± 0.48	19.1 ± 7.44	1.48 ± 0.336
Mizunara (MZ, <i>Quercus crispula</i> Blume)	40/120	40/60/80	6	732 ± 59.7	12.4 ± 0.91	42.8 ± 27.2	2.32 ± 0.931
Buna (BN, <i>Fagus crenata</i> )	40/120	40/60/80	6	687 ± 17.8	12.9 ± 0.31	55.6 ± 18.3	2.99 ± 0.515

a) Number of specimens, b) density, c) the values mean average ± standard variation, d) moisture content, e) angle of annual rings, f) average of annual ring width



**Fig. 1** Schematic of partial compression test perpendicular to the grain (dimensions in mm) [1]

A tensile and compression testing machine (MAEKAWA MFG. CO., LTD. A-300-B4) was used for the loading. The vertical displacements of the bearing metal plate were measured at two points using displacement transducers (Tokyo Measuring Instruments Laboratory Co., Ltd., CDP-25), and the average value was considered the test displacement. The ratio of displacement to height was considered the test strain. The load is measured using a test machine. The load divided by the loading area (1600 mm<sup>2</sup>) was considered the test stress. The elastic stiffness ( $E_e$ ), plastic stiffness ( $E_p$ ), yield stress

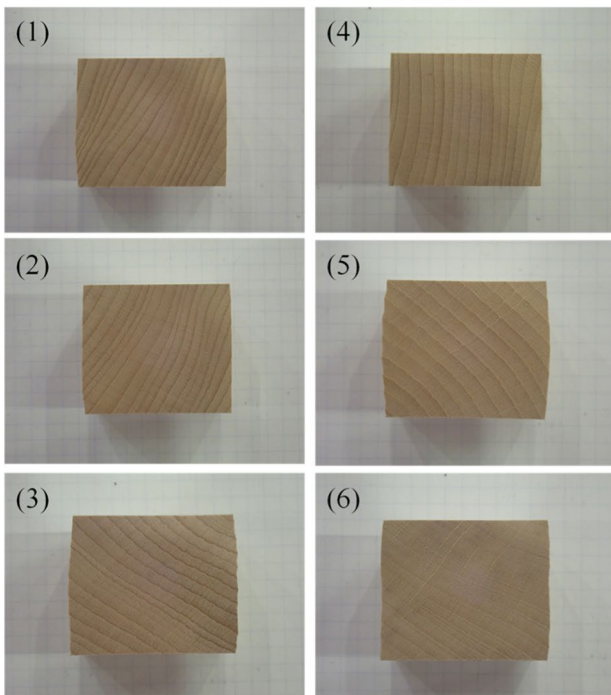
( $\sigma_y$ ), and yield strain ( $\varepsilon_y$ ) were calculated from the stress–strain curves.  $E_e$  was calculated following Inayama’s study [3], and  $E_p$ ,  $\sigma_y$  and  $\varepsilon_y$  were calculated following Fujita’s study [7].

## Results and discussion

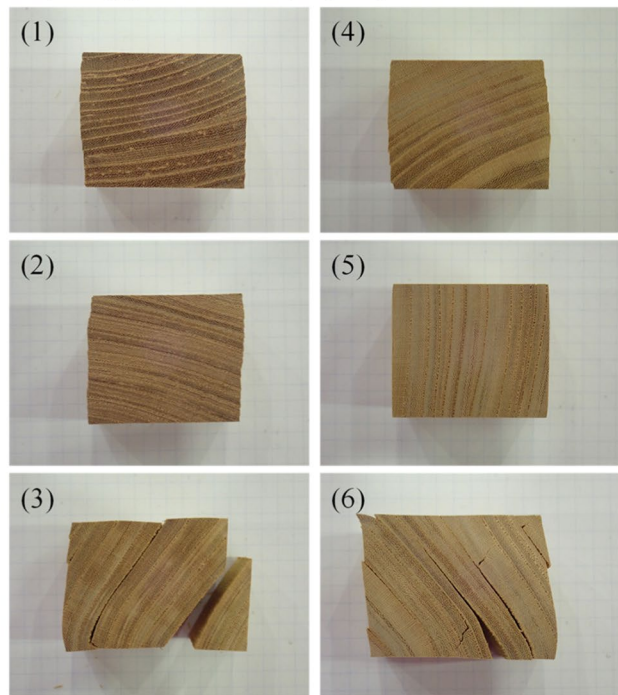
### Fracture morphology

Figure 2 shows the fracture morphologies of the diffuse-porous wood (buna) and ring-porous wood (keyaki) in the full compression test (4040). Buna and keyaki were selected because they were considered to represent the typical fracture morphologies of diffuse- and ring-porous wood, respectively. In the full compression test, the fracture morphology differed depending on the porous structure and the annual ring in the direction of the load (AAR). The AARs are classified as close to 0° [see Fig. 2A (3), (6), B(1), (2), and (4)], close to 45° [see Fig. 2A (5), B(3), and (6)], and close to 90° [see Fig. 2A(1), (2), (4), and B(5)]. For all specimens, in addition to deformation in the direction of the applied load, deformation was first observed in a direction approximately orthogonal to the direction of the applied load due to the Poisson effect. The cracking and fracture of specimens occurred as the deformation progressed. In diffuse-porous wood, the Poisson effect causes swelling deformation around the centre of the height of the specimen. The shape of the deformation varied slightly owing to the AAR and

A ) Diffuse-porous wood (Buna)



B ) Ring-porous wood (Keyaki)



**Fig. 2** Fracture morphologies of full compression test specimen (4040) for diffuse- and ring-porous woods

the bending of the annual ring. No visible cracks or fractures were present except in Shirakashi. This seems to be caused by the radial arrangement of the vessels and large rays in Shirakashi. Similar to diffuse-porous wood, the Poisson effect in ring-porous wood causes swelling deformation around the centre of the height of the specimen. However, in contrast to the diffuse-porous wood, shear and compression failures of the pore zone and cracks caused by these failures were observed. Such cracks were observed more frequently in Kuri and Keyaki, particularly in specimens with an AAR close to  $45^\circ$ , and less frequently in specimens with an AAR close to  $0^\circ$  or those with an ARA close to  $90^\circ$  and straight annual rings. No cracks were observed in Yachidamo. Some Mizunara specimens showed cracks in the radial direction, which may have been owing to large rays similar to those of Shirakashi.

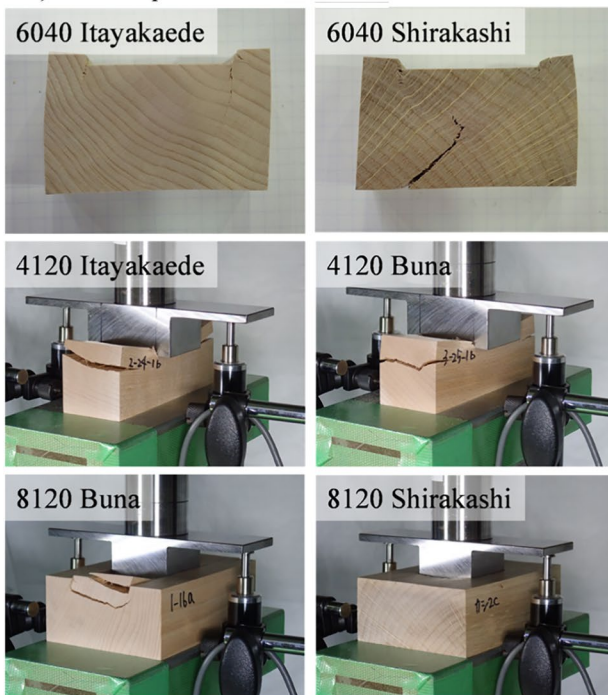
Figure 3 shows the fracture morphologies of diffuse and ring-porous wood in the partial compression test (6040, 8040, 4120, and 8120). The next clearest difference in the fracture morphology owing to the porous structure was observed in the specimens with an edge distance only orthogonal to the longitudinal direction (6040 and 8040). In these specimens, cracks first appeared at the edges of the loading area in both the diffuse- and ring-porous woods. Subsequently, in ring-porous wood,

these cracks led to fractures along the pore zone. In some specimens, the Poisson effect causes swelling and cracking at the bottom of the specimen. In the specimen with an edge distance parallel to the grain (4120), there was little difference in the fracture morphology owing to the porous structure, whereas, in the specimen with an edge distance only parallel to the grain, nearly all specimens showed shear failure at the edge of the loading area and cracking at the end of the specimens. In addition, in specimens with edge distances parallel and perpendicular to the grain (6120 and 8120), shear failure at the edge of the loading area was observed in all specimens and cracking at the end of the specimen within the width of the loading area was observed in many specimens.

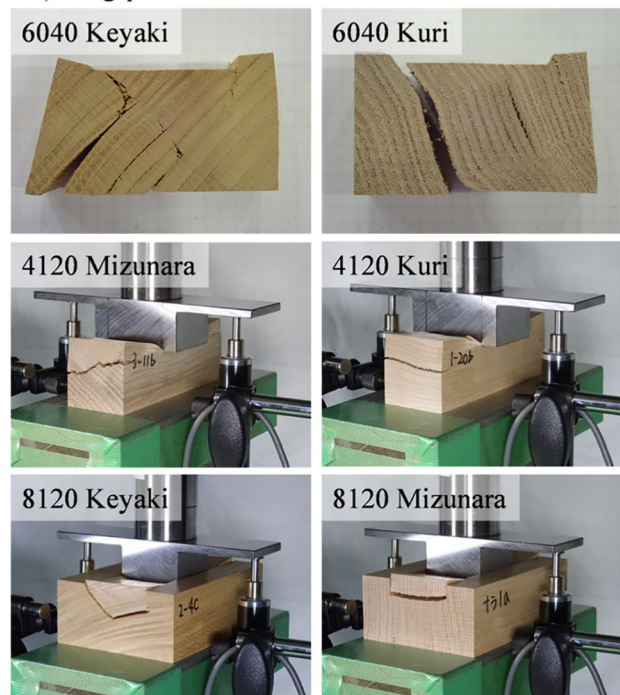
### Stress–strain curve

Figure 4 shows the stress–strain curves of the compression test perpendicular to the grain for diffuse-porous wood (Buna) and ring-porous wood (Keyaki). Buna and Keyaki were selected because they were considered to represent the typical behaviors of the curves of diffuse- and ring-porous wood, respectively. The curves are to the point of maximum stress. For both diffuse- and ring-porous wood, the stress–strain curves of the specimen with a length of 120 mm showed a drop in stress between

#### A ) Diffuse-porous wood



#### B ) Ring-porous wood



**Fig. 3** Fracture morphologies of partial compression test (6040, 8040, 4120, 6120, and 8120) specimen for diffuse- and ring-porous woods. The four-digit numbers 4120, 6040, 6120, 8040, and 8120 represent dimensional specifications as shown in Table 2

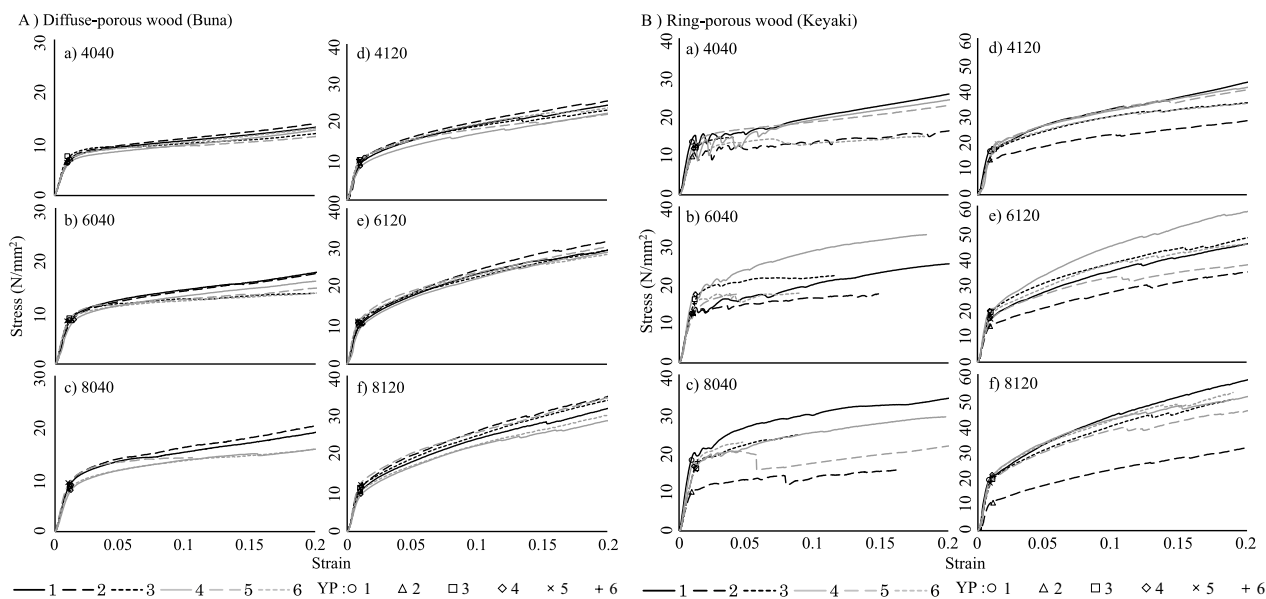


**Fig. 4** Stress–strain curves of compression test perpendicular to the grain for diffuse- and ring-porous woods. The four-digit numbers 4040, 4120, 6040, 6120, 8040, and 8120 represent dimensional specifications. YP: Yield point. The curves are to the point of maximum stress. The numbers in the figure legend represent the identification number of the specimen as in Fig. 2

the strain of 0.07 and 0.15. This is caused by cracking at the end of the specimen.

In diffuse-porous wood, a gradual decrease in stiffness was observed after the yield point in all specifications. The ring-porous wood had a clearer tendency to a decrease in stiffness than in the diffuse-porous wood with the same dimensions at the yield point. In the specification without edge distance (4040) of the diffuse-porous wood, the load increased and decreased repeatedly after the yield point [1]. Furthermore, more ring-porous wood specimens showed a significant drop in load before reaching a strain of 0.2, compared with the diffuse-porous wood specimens. This behaviour may be due to the sequential failure of vessels in the pore zone of the ring-porous wood [1]. In Fig. 4, ring-porous wood (Keyaki) (5) did not show these behaviours, which may be owing to the fact that the AAR was close to 90° and the annual rings were linear; therefore, less failure occurred in the pore zone.

The load increase/decrease ratios were smaller for specifications with edge distance than those without edge distance [1]. The load increase/decrease behaviour was less apparent for specifications with an edge distance parallel to the grain (4120, 6120, and 8120) [1]. This shows that the edge distance constrained the fracture of vessels in the pore zone [1]. For the edge distance perpendicular to the grain, shear failure occurred at the edge of the loading area, which may have weakened this effect compared to the edge distance parallel to the grain [1].

**Relationship between the characteristic values and density [1]**

Table 2 summarises the characteristic values of partial compression test perpendicular to the grain for each specification. Figure 5 shows the relationship between characteristic values and the density of each dimensional specification and represents the regression line calculated for each dimensional specification for the relationships between  $E_e$  and density and  $\sigma_y$  and density.

For  $E_e$  and  $\sigma_y$ , a significant positive correlation was observed ( $p < 0.01$ ) with density for all dimensional specifications. In both cases, the correlation is stronger in specifications with edge distance than in those without. Furthermore, the slope of the regression line increased with the edge distance, both parallel and perpendicular to the grain. However, little difference was observed in the slope of the line between the specimens with widths of 60 and 80 mm. A possible explanation for this is that the effects of factors other than density, such as the annual ring angle, were less affected by the partial compression specifications because the deformation was constrained by the edge distance. For  $\sigma_y$ , the correlation was stronger than that for  $E_e$  for all dimensional specifications. The effect of density may have been greater for  $\sigma_y$  than for  $E_e$ , while the effects of other factors may have been relatively less. However, there was no clear difference between the diffuse- and ring-porous wood.

**Table 2** Results of partial compression test perpendicular to the grain [1]

W.S	Size	$E_e^{a,b}$ (kN/mm <sup>2</sup> )	$E_p^{b,c}$ (kN/mm <sup>2</sup> )	$\sigma_y^{b,d}$ (N/mm <sup>2</sup> )	$\varepsilon_y^{b,e}$ (%)
IT	4040	1.52 (0.146)	0.088 (0.016)	14.3 (1.79)	1.07 (0.071)
	6040	1.82 (0.277)	0.137 (0.028)	17.3 (2.93)	1.04 (0.069)
	8040	1.88 (0.214)	0.167 (0.019)	17.3 (1.29)	1.01 (0.081)
	4120	2.27 (0.209)	0.215 (0.025)	18.9 (2.18)	0.92 (0.065)
	6120	2.64 (0.284)	0.267 (0.034)	20.7 (2.54)	0.85 (0.039)
	8120	2.69 (0.273)	0.288 (0.041)	21.2 (1.89)	0.91 (0.099)
SR	4040	1.29 (0.194)	0.138 (0.006)	13.3 (1.57)	1.12 (0.032)
	6040	1.75 (0.231)	0.214 (0.006)	16.9 (1.70)	1.12 (0.107)
	8040	1.76 (0.031)	0.252 (0.024)	17.1 (0.36)	1.11 (0.027)
	4120	1.94 (0.284)	0.283 (0.038)	18.9 (1.95)	1.06 (0.069)
	6120	2.61 (0.212)	0.386 (0.045)	21.3 (2.20)	0.92 (0.125)
	8120	2.41 (0.012)	0.403 (0.031)	22.7 (2.17)	1.05 (0.103)
UD	4040	1.00 (0.284)	0.057 (0.011)	10.4 (1.98)	1.15 (0.098)
	6040	1.40 (0.079)	0.078 (0.003)	13.0 (0.74)	1.01 (0.078)
	8040	1.25 (0.051)	0.120 (0.022)	12.6 (0.27)	1.11 (0.065)
	4120	1.52 (0.376)	0.164 (0.017)	13.7 (2.32)	1.04 (0.047)
	6120	2.11 (0.081)	0.198 (0.024)	15.9 (0.72)	0.84 (0.041)
	8120	2.02 (0.163)	0.229 (0.024)	16.3 (0.94)	0.90 (0.050)
KR	4040	0.88 (0.480)	0.024 (0.011)	5.15 (1.62)	0.72 (0.211)
	6040	1.04 (0.517)	0.036 (0.025)	6.26 (2.20)	0.76 (0.197)
	8040	1.04 (0.349)	0.040 (0.028)	6.46 (1.55)	0.77 (0.106)
	4120	1.24 (0.411)	0.085 (0.026)	6.91 (1.47)	0.65 (0.109)
	6120	1.49 (0.522)	0.113 (0.041)	7.15 (1.90)	0.57 (0.081)
	8120	1.47 (0.479)	0.127 (0.030)	7.63 (1.72)	0.66 (0.109)
KY	4040	1.44 (0.267)	0.073 (0.034)	12.0 (1.25)	0.98 (0.135)
	6040	1.67 (0.192)	0.116 (0.052)	14.5 (2.15)	0.98 (0.092)
	8040	1.85 (0.387)	0.153 (0.045)	15.7 (2.96)	1.00 (0.146)
	4120	1.89 (0.278)	0.200 (0.040)	17.0 (2.09)	1.04 (0.188)
	6120	2.39 (0.342)	0.263 (0.053)	17.3 (2.12)	0.83 (0.036)
	8120	2.50 (0.466)	0.294 (0.062)	18.4 (3.92)	0.87 (0.077)
YC	4040	0.95 (0.172)	0.004 (0.010)	5.86 (0.84)	0.71 (0.035)
	6040	1.04 (0.236)	0.025 (0.017)	6.66 (0.93)	0.72 (0.062)
	8040	1.08 (0.208)	0.032 (0.015)	6.73 (0.51)	0.74 (0.078)
	4120	1.32 (0.239)	0.068 (0.032)	7.30 (0.82)	0.67 (0.041)
	6120	1.53 (0.243)	0.093 (0.040)	7.38 (0.76)	0.58 (0.037)
	8120	1.54 (0.212)	0.101 (0.030)	7.85 (1.01)	0.63 (0.052)
MZ	4040	1.02 (0.294)	0.040 (0.013)	8.67 (1.93)	0.95 (0.084)
	6040	1.29 (0.418)	0.064 (0.012)	10.6 (3.27)	0.92 (0.075)
	8040	1.26 (0.373)	0.096 (0.017)	11.4 (3.59)	0.99 (0.057)
	4120	1.52 (0.357)	0.152 (0.050)	11.4 (2.81)	0.85 (0.052)
	6120	1.89 (0.537)	0.193 (0.051)	12.4 (3.85)	0.75 (0.063)
	8120	1.92 (0.463)	0.228 (0.060)	13.4 (3.87)	0.81 (0.047)
BN	4040	0.79 (0.069)	0.072 (0.013)	6.77 (0.52)	0.95 (0.079)
	6040	0.97 (0.138)	0.097 (0.012)	8.43 (0.26)	0.99 (0.181)
	8040	1.04 (0.129)	0.124 (0.014)	8.70 (0.61)	0.98 (0.071)
	4120	1.20 (0.124)	0.143 (0.007)	9.92 (0.76)	0.94 (0.128)
	6120	1.43 (0.240)	0.190 (0.012)	10.6 (0.46)	0.86 (0.144)
	8120	1.43 (0.235)	0.192 (0.013)	10.9 (1.00)	0.90 (0.072)

W.S.: wood species, a) elastic stiffness, b) mean average (standard deviation), c) plastic stiffness, d) yield stress, e) yield strain; size shows the dimensional specifications

**Effect of edge distance on the increased ratios of characteristic values [1]**

Figure 6 shows the relationship between the increased ratios of  $E_e$  and  $\sigma_y$  and the edge distance perpendicular to the grain. The increased ratios of  $E_e$  and  $\sigma_y$  are defined as the average of the ratio of the characteristic value of a specimen to that of the full compression specimen without both edge distances being prepared from the same material.

As shown in Fig. 6, the increased ratios of  $E_e$  and  $\sigma_y$  were higher for the partial compression specimens than for the full compression specimens. Irrespective of the edge distance parallel to the grain (0 or 40 mm), the increased ratios of  $E_e$  and  $\sigma_y$  tended to increase with the increase in the edge distance perpendicular to the grain. By contrast, at an edge distance perpendicular to the grain longer than 10 mm, the increased ratios of  $E_e$  and  $\sigma_y$  increased only slightly or remained constant depending on the wood species. This suggests that the effect of the edge distance parallel to the grain on the improvement of the characteristic values converges. These trends agree with those reported in a previous study on softwood by Inayama [3].

As shown in Fig. 6, the increased ratios of  $E_e$  and  $\sigma_y$  tended to be higher for Shirakashi and Udaikamba and lower for Yachidamo compared to other species. These results suggest that there are differences among wood species. Figure 7 shows the relationship between the increase in the ratio of the characteristic values and the density. For each dimensional specification, there was little significant relationship between the increased ratio of  $E_e$  and  $\sigma_y$  and density. Similar results were obtained when the samples were divided into diffuse- and ring-porous woods. This suggests that the increased ratio of characteristic values independent of density and factors other than density, or whether the wood is diffuse- or ring-porous, may be responsible for the differences between wood species. Therefore, further studies are needed to clarify the effects of annual ring angles and other factors.

**Relationships between characteristic values [1]**

Figures 8 and 9 show the relationships between  $E_e$  and  $E_p$  and  $\sigma_y$  and  $\varepsilon_y$ , respectively, and indicate that both relationships are significantly positively correlated. However, the relationships between  $\sigma_y$  and  $\varepsilon_y$  had a smaller correlation coefficient than  $E_e$  and  $E_p$  and were not strongly correlated. Figure 9 shows that a positive correlation between  $\sigma_y$  and  $\varepsilon_y$ . However, this relationship might differ for each wood species.

Table 3 summarises the linear regression equations calculated for each wood species, the dimensional specifications for the relationships between  $E_e$  and  $E_p$ ,  $\sigma_y$  and  $\varepsilon_y$ , and their coefficients of determination. Significant

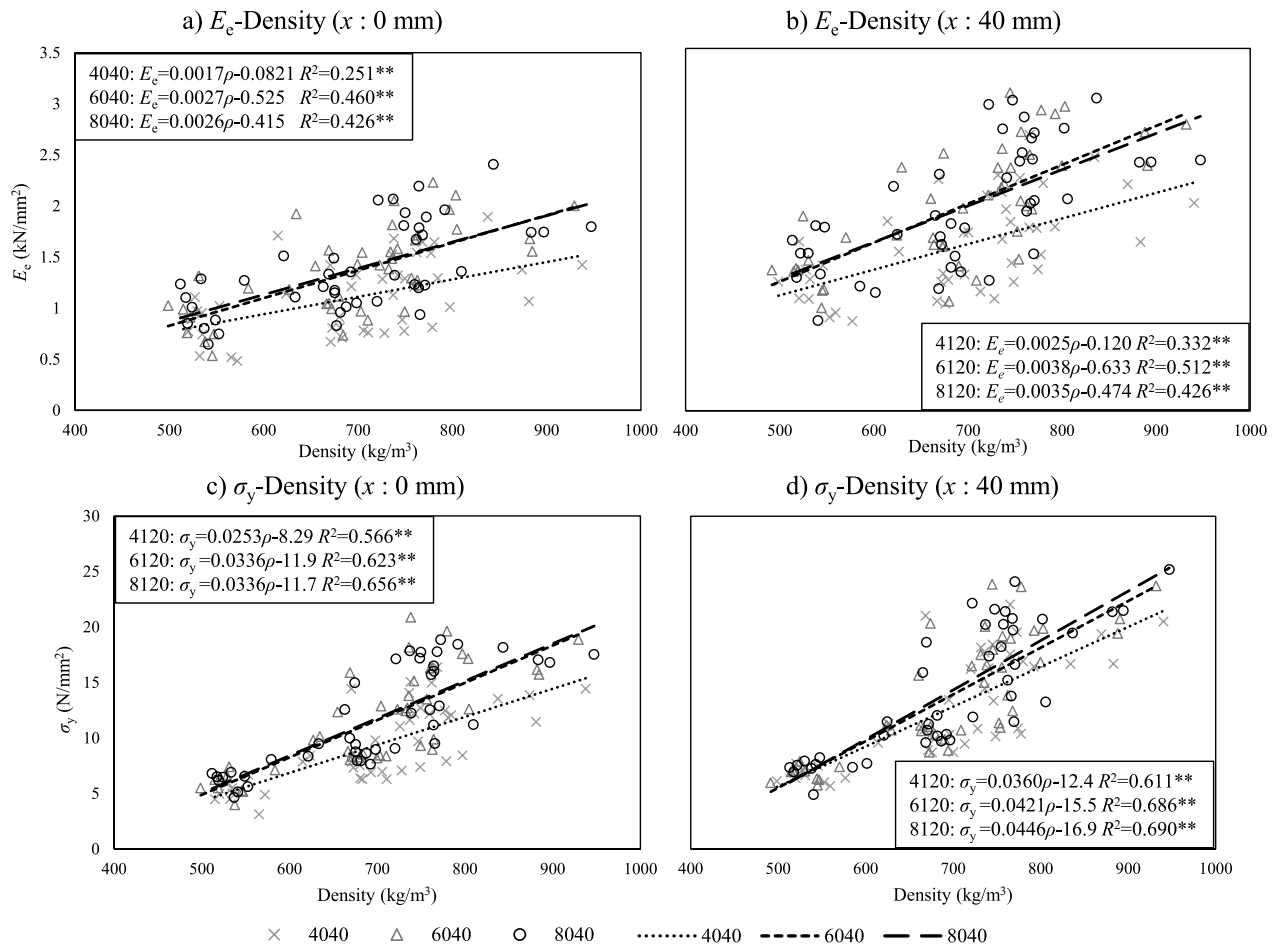


**Fig. 5** Relationship between characteristic values and density of each dimensional specification in all specimens [1].  $E_c$ : elastic stiffness,  $x$ : edge distance parallel to the grain,  $\rho$ : density,  $R^2$ : coefficient of determination,  $\sigma_y$ : yield strength, 4040, 6040, 8040, 4120, 6120 and 8120: dimensional specifications, \*: significant at 5% level, \*\*: significant at 1% level

positive correlations were observed between  $E_e$  and  $E_p$  for all wood species and dimensional specifications. Therefore, a positive correlation existed between the elastic and plastic stiffness in the compression strength of wood perpendicular to the grain, regardless of the wood species and dimensional specifications. For the dimensional specifications, the slope and coefficient of determination of the linear regression equation were the smallest for the full compression specification (4040), and each value increased with increasing edge distance perpendicular to the grain. In addition, they tended to be larger for specifications with an edge distance parallel to the grain. This slope occurred because the plastic stiffness was close to zero for the full compression specification (4040) and the stiffness increased with increasing edge distance. The coefficient of determination was due to the constraining effect of the edge distance on the deformation and fracture of the specimens, which reduced the variation

between the elastic and plastic stiffnesses. In the relationship between  $\sigma_y$  and  $\varepsilon_y$ , significant positive correlations were found for each dimensional specification; however, significant negative, negative and positive correlations were found for IT, SR, UD, KR and YC, MZ and BN and KY, respectively. Previous studies on softwoods [3] and hardwoods [7] have shown that for the same species, loading area dimensions and specimen height, relationships between  $\sigma_y$  and  $\varepsilon_y$  are inversely related. This may also be true for the results of this study, as the relationship is not clear but is close to inversely proportional when the same wood species, loading area dimensions, and specimen height are held constant. However, the relationship between  $\sigma_y$  and  $\varepsilon_y$  was significantly positively correlated for each dimensional specification. Although the coefficient of determination was smaller than that in the relationship between  $E_e$  and  $E_p$ , the slope and coefficient of determination in the relationship between  $\sigma_y$  and

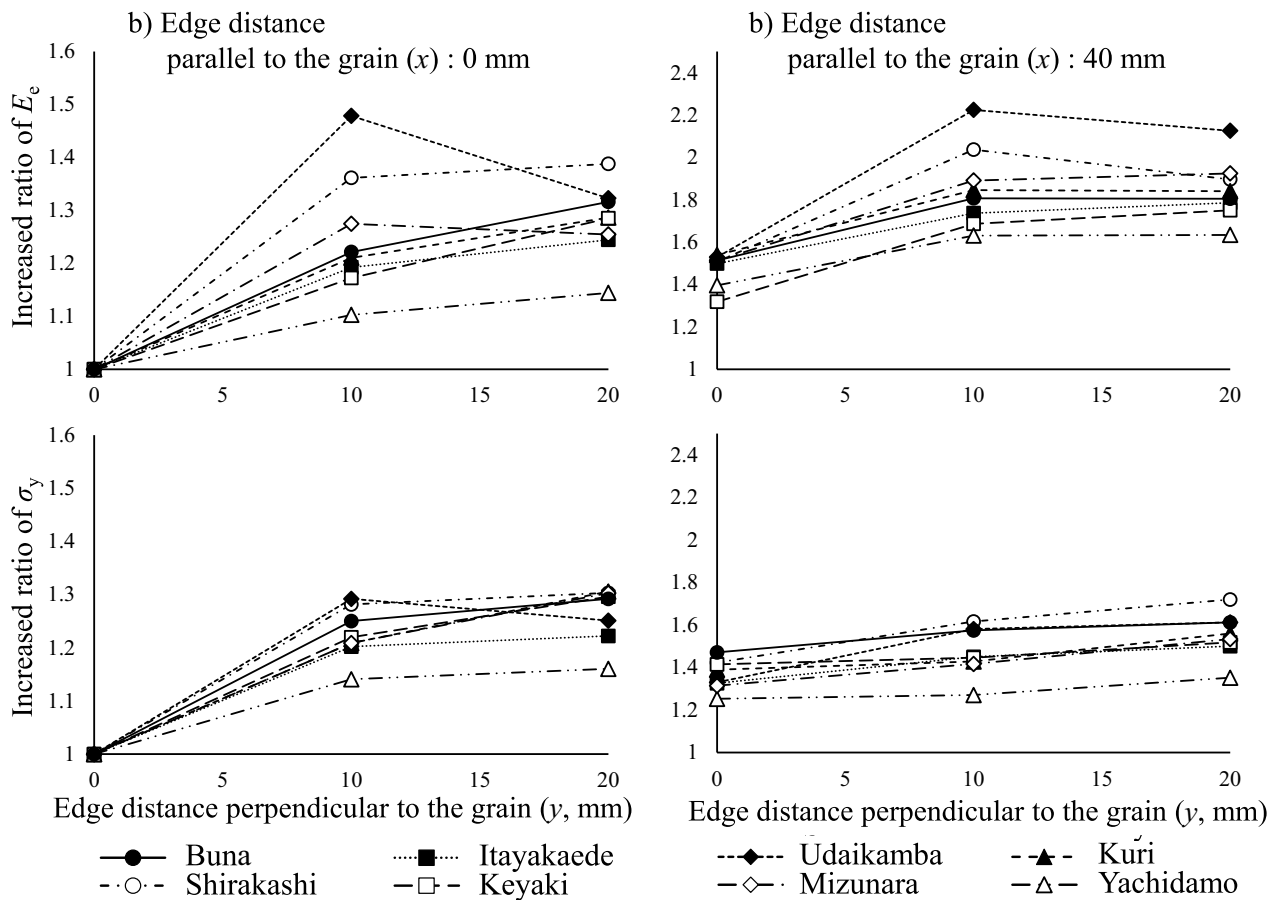


**Fig. 6** Relationships between the increased ratio of characteristic values and edge distance perpendicular to the grain [1]. See Fig. 5

$\epsilon_y$  were similar to those in the relationship between  $E_e$  and  $E_p$ . These results suggest that a positive correlation exists between  $\sigma_y$  and  $\epsilon_y$  for dimensional specifications regardless of the species.

**Conclusion**

The aim of this study was to investigate the effect of the edge distance parallel and perpendicular to the grain and wood species on the compression performance of hardwoods perpendicular to the grain. The results of this study are as follows:

1. Fracture morphologies showed the greatest difference between diffuse- and ring-porous wood in the full compression test, and the difference decreased with increasing edge distance, especially parallel to the grain.
2. The behaviour of the stress–strain curve after the yield point may differ depending on the porous structure [1].

3. With respect to the edge distance parallel to the grain, the variations in the elastic stiffness and yield stress can be reduced by constraining the deformation and fracture with the edge distance perpendicular to the grain [1].
4. The elastic stiffness and yield stress were significantly correlated with the density, and the specifications with an edge distance perpendicular, parallel, or both to the grain had a stronger correlation than those without it [1].
5. The effect of the edge distance perpendicular to the grain on the increased ratio of elastic stiffness and yield stress tends to be similar to that of softwood [3] and may vary between wood species [1].
6. It is suggested that factors other than density and whether wood is diffuse- or ring-porous are responsible for the differences in the increase ratio of elastic stiffness and yield stress between wood species.
7. The relationships between the elastic stiffness and plastic stiffness, yield stress and yield strain tend to be similar to those for softwood [1].



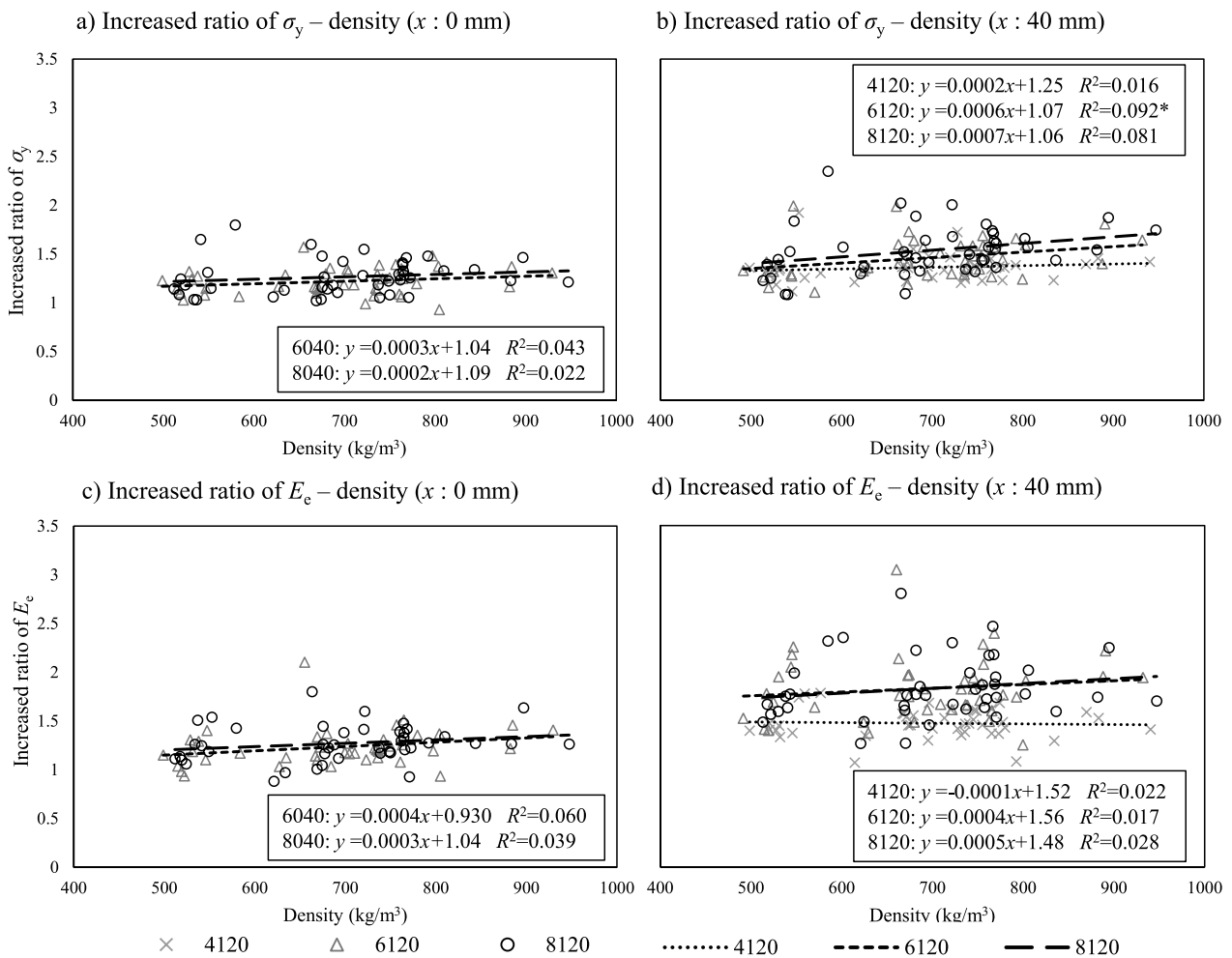


**Fig. 7** Relationship between increased ratio of characteristic values and density of each specimen. See Fig. 5

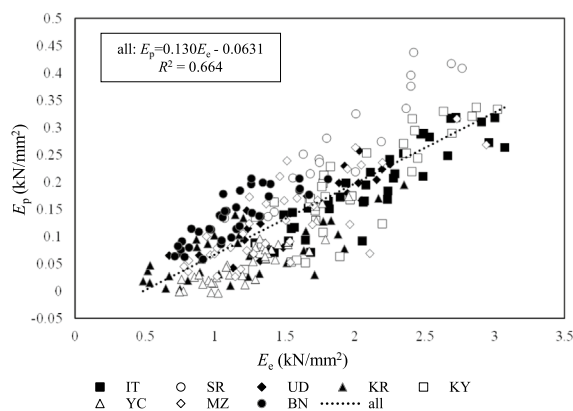


**Fig. 8** Relationship between  $E_e$  and  $E_p$  in all specimens [1]. iu.  $E_p$ , plastic stiffness;  $E_e$ , elastic stiffness; IT Itayakaede; SR, Shirakashi; UD, Udaikamba; KR, Kuri; KY, Keyaki; YC, Yachidamo; MZ, Mizunara; BN, Buna;  $R^2$ , coefficient of determination

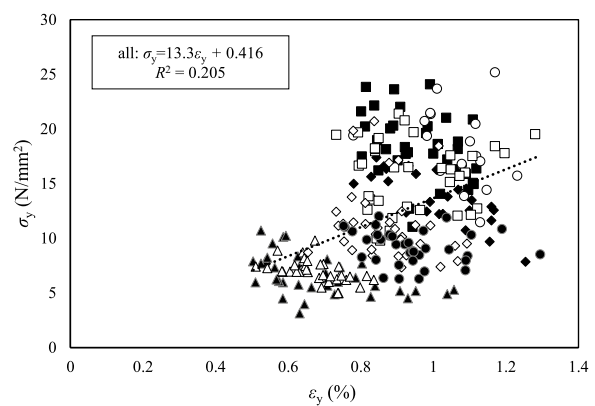


**Fig. 9** Relationship between  $\sigma_y$  and  $\epsilon_y$  in all specimens [1].  $\sigma_y$ , yield strength;  $\epsilon_y$ , yield strain; IT, Itayakaede; SR, Shirakashi; UD, Udaikamba; KR, Kuri; KY, Keyaki; YC, Yachidamo; MZ, Mizunara; BN, Buna;  $R^2$ , coefficient of determination

**Table 3** Results of correlation analysis for each specification in the relationship between characteristic values [1]

	Relationship between $E_e$ and $E_p$		Relationship between $\sigma_y$ and $\varepsilon_y$	
	The linear regression equation	$R^2$	The linear regression equation	$R^2$
IT	$E_p = 0.139E_e - 0.103$	0.806**	$\sigma_y = -12.2\varepsilon_y + 30.0$	0.165*
SR	$E_p = 0.193E_e - 0.0981$	0.875**	$\sigma_y = -10.7\varepsilon_y + 29.7$	0.0948**
UD	$E_p = 0.123E_e - 0.0493$	0.701**	$\sigma_y = -14.7\varepsilon_y + 28.5$	0.606**
KR	$E_p = 0.0658E_e - 0.00741$	0.451**	$\sigma_y = -5.84\varepsilon_y + 10.6$	0.234**
KY	$E_p = 0.160E_e - 0.130$	0.747**	$\sigma_y = 1.61\varepsilon_y + 14.3$	0.00464
YC	$E_p = 0.125E_e - 0.101$	0.791**	$\sigma_y = -6.65\varepsilon_y + 11.5$	0.253**
MZ	$E_p = 0.119E_e - 0.0472$	0.604**	$\sigma_y = -5.56\varepsilon_y + 16.2$	0.0285
BN	$E_p = 0.134E_e - 0.0175$	0.681**	$\sigma_y = -2.72\varepsilon_y + 11.8$	0.0437
4040	$E_p = 0.0404E_e + 0.0124$	0.141*	$\sigma_y = 11.9\varepsilon_y - 1.89$	0.373**
4120	$E_p = 0.110E_e - 0.0202$	0.551**	$\sigma_y = 18.9\varepsilon_y - 3.99$	0.465**
6040	$E_p = 0.0812E_e - 0.0206$	0.380**	$\sigma_y = 15.8\varepsilon_y - 3.31$	0.339**
6120	$E_p = 0.123E_e - 0.0404$	0.646**	$\sigma_y = 26.3\varepsilon_y - 6.55$	0.465**
8040	$E_p = 0.106E_e - 0.0317$	0.492**	$\sigma_y = 18.0\varepsilon_y - 5.43$	0.356**
8120	$E_p = 0.128E_e - 0.0314$	0.641**	$\sigma_y = 27.3\varepsilon_y - 8.34$	0.458**

$E_e$ , elastic stiffness;  $E_p$ , plastic stiffness;  $\sigma_y$ , yield strength;  $\varepsilon_y$ , yield strain; IT, Itayakaede; SR, Shirakashi; UD, Udaikamba; KR, Kuri; KY, Keyaki; YC, Yachidamo; MZ, Mizunara; BN, Buna

$R^2$  shows coefficient of determination, \*\* significant at  $p < 0.01$ , \* significant at  $p < 0.05$

These results support the possibility of estimating the partial compression performance of hardwoods perpendicular to the grain as softwood [1]. However, some species showed greater variability in their characteristic values, particularly for ring-porous wood [1]. More detailed studies are needed on the effects of different species, especially on the porous structure and the effects of the annual ring inclination angle [1].

#### Abbreviations

IT	Itayakaede ( <i>Acer mono</i> Maxim.)
UD	Udaikamba ( <i>Betula maximowicziana</i> )
BN	Buna ( <i>Fagus crenata</i> )
SR	Shirakashi ( <i>Quercus myrsinifolia</i> )
KR	Kuri ( <i>Castanea crenata</i> )
KY	Keyaki ( <i>Zelkova serrata</i> )
YC	Yachidamo ( <i>Fraxinus mandshurica</i> )
MZ	Mizunara ( <i>Quercus crispula</i> Blume)
AAR	Angle of an annual ring of specimen in the test load direction

#### Acknowledgements

Part of this report was presented at the Annual Meeting of Architectural Institute of Japan Hokkaido 2022 in September 2022 and at the 13th World Conference on Timber Engineering 2023 in June 2023.

#### Author contributions

All the authors designed the experiments. HS performed the experiments, analysed the data, and was a major contributor to writing the manuscript. All the authors contributed to the interpretation and discussion of the results. All the authors have read and approved the final version of the manuscript.

#### Funding

This work was supported by JSPS Grant-in-Aid for Early-Career Scientists Grant Number JP20K15572, and by the International Exchange Encouragement Award from the Japan Wood Research Society through JSPS Grants-in-Aid for Publication of Scientific Research Results Grant Number JP22HP2003.

#### Availability of data and materials

The data sets used and analysed in the current study are available from the corresponding author upon reasonable request.

#### Declarations

#### Competing interests

The authors declare that they have no competing interests.

Received: 22 December 2023 Accepted: 24 June 2024

Published online: 19 September 2024

#### References

- Suesada H, Miyamoto K (2023) Experimental study on characteristic values of partial compression perpendicular to the grain of hardwood with edge distance orthogonal to the longitudinal direction. In: World conference on timber engineering (WCTE 2023). p. 147–152. <https://doi.org/10.52202/069179-0020>
- Forestry Agency (2023) Annual report on forest and forestry in Japan Fiscal year 2022 (Summary). <https://www.rinya.maff.go.jp/j/kikaku/hakusyo/r4hakusyo/attach/pdf/index-6.pdf>. Accessed 8 Dec 2023.
- Inayama M (1991) Wooden embedment theory and its application. Dissertation, The University of Tokyo. (in Japanese)
- Inayama M (1992) Study on compression perpendicular to the grain in wood part 3:  $E_1$ ,  $E_2$  and  $\sigma_y$  under the influence of thickness, end distances, edge distances and lengths of compression area. In: Summaries of technical papers of annual meeting, C-II: 13–14, Architectural Institute of Japan, 1992. (in Japanese)
- Inayama M (1993) Study on compression perpendicular to the grain in wood part 4: analytic functions for the relation between compression load and elastic deformation perpendicular to the grain in wood. In: Summaries of technical papers of annual meeting, C-II:907–908, Architectural Institute of Japan; 1993. (in Japanese)
- Architectural Institute of Japan (2009) Design manual for engineered timber joints. Architectural Institute of Japan, Tokyo
- Fujita K, Inayama M, Ando N (2012) Embedding performance of Four kinds of domestic hard wood used as wooden dowels. *Mokuzai Gakkaishi* 58(4):181–192. <https://doi.org/10.2488/jwrs.58.181>. (in Japanese)
- JIS Z 2101 (2009) Methods of test for woods. Japanese Standards Association, Tokyo

#### Publisher's Note

Springer Nature remains neutral with regard to jurisdictional claims in published maps and institutional affiliations.